

The DIRC detectors of the PANDA experiment at FAIR

Klaus Föhl,^{a,*} Diego Bettoni,^b Derek Branford,^a Alexander Britting,^c Vittore Carassiti,^b
Annalisa Cecchi,^b Valery Kh. Dodokhof,^d Michael Düren,^e Markus Ehrenfried,^e
Wolfgang Eyrich,^c Derek Glazier,^a Matthias Hoek,^f Roland Hohler,^g Ralf Kaiser,^f
Albert Lehmann,^c Dorothee Lehmann,^g Shaojun Lu,^e Johann Marton,^h Oliver Merle,^e
Klaus Peters,^g Cecilia Pizzolotto,^c Günther Rosner,^f Georg Schepers,^g Roland Schmidt,^e
Lars Schmitt,^g Peter Schönmeier,^e Carsten Schwarz,^g Björn Seitz,^f Concettina Sfienti,^g
Ken Suzuki,^h Andreas Teufel,^c Alexandre S. Vodopianov,^d Daniel Watts^a

^a*School of Physics, University of Edinburgh, Mayfield Road, Edinburgh EH9 3JZ, Scotland, UK*

^b*INFN Ferrara, Via Paradiso 12, I-44100 Ferrara, Italy*

^c*Physikalisches Institut IV, University of Erlangen-Nuremberg, Erlangen, Germany*

^d*Laboratory of High Energies, Joint Institute for Nuclear Research, 141980 Dubna, Russia*

^e*II Physikalisches Institut, University of Giessen, Giessen, Germany*

^f*Department of Physics & Astronomy, Kelvin Building, University of Glasgow, Glasgow G12 8QQ, Scotland, UK*

^g*Gesellschaft für Schwerionenforschung mbH, Planckstraße 1, 64291 Darmstadt, Germany*

^h*Stefan Meyer Institut für subatomare Physik, Austrian Academy of Sciences, A-1090 Vienna, Austria*

Abstract

The PANDA experiment at the future Facility for Anti-proton and Ion Research (FAIR) aims at studying strong interaction with antiprotons in the 1–15 GeV/c range. For the charged particle identification, in particular kaons, one foresees three imaging Cherenkov detectors. Two DIRC detectors will be located in the target spectrometer section of PANDA, one a barrel shape DIRC with bar radiators in the centre part, and a disc DIRC in the forward endcap part. For the latter, two readout concepts are investigated: measuring the photons' time-of-propagation in a multi wavelength band disc DIRC, or measuring angles in a focussing lightguide dispersion-correcting disc DIRC.

Key words: Particle identification, Cherenkov counter, ring imaging

PACS: 29.40.Ka

1 The PANDA¹ experiment [1] at the future FAIR 9
2 laboratory is a fixed target experiment scattering 10
3 cooled antiprotons circulating in the High Energy 11
4 Storage Ring (HESR) with momenta of 1-15 GeV/c 12
5 off an internal pellet or gas jet target at interac- 13
6 tion rates of up to $2 \cdot 10^7/s$ to perform high preci- 14
7 sion experiments in the charmed quark range. The 15
8 target spectrometer section with a superconducting 16
9 solenoid and most subdetectors housed inside a re- 17
10 turn yoke covers the acceptance except for a hole of
11 $\vartheta=10^\circ$ horizontal and $\vartheta=5^\circ$ vertical in the forward
12 direction opening towards a dipole providing addi-
13 tional bending power and the subdetectors of the
14 forward spectrometer section.
15 Three imaging Cherenkov detectors are foreseen
16 for the charged particle identification of the PANDA
17 experiment, two of them are DIRCs². For parti-

* corresponding author

Email address: kf@ph.ed.ac.uk (Klaus Föhl).

¹ antiProton ANnihilation at DArmstadt

² Detector of Internally Reflected Cherenkov light

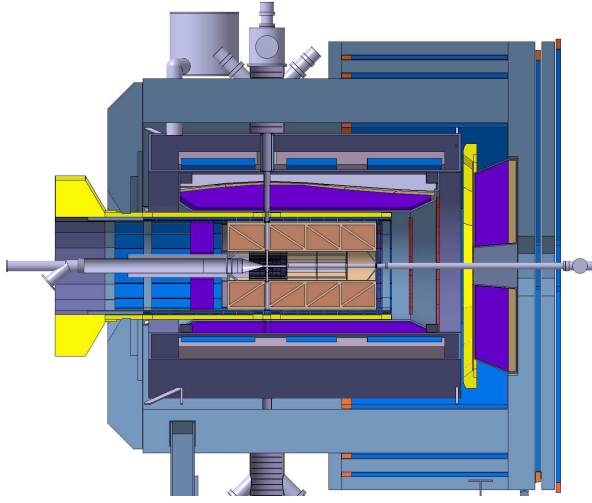


Fig. 1. PANDA target spectrometer. The Barrel and the Endcap DIRC detector positions are shown in light colour.

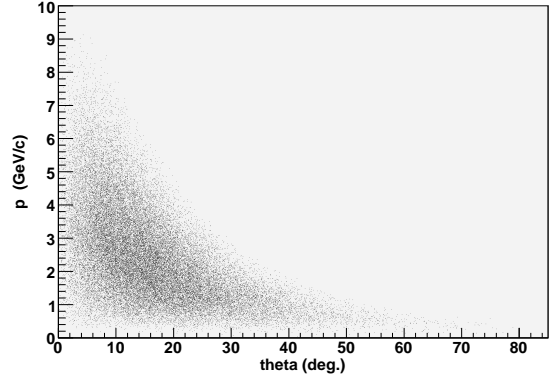


Fig. 2. Acceptance plot for kaons from the $p\bar{p} \rightarrow \psi_h \eta$ reaction at $p_{\bar{p}}=15$ GeV/c. The Barrel DIRC covers the range $\vartheta=22^\circ-140^\circ$, the Endcap DIRC the more forward range $\vartheta=5^\circ-22^\circ$.

cle identification their information will be combined with adjacent tracking and calorimetry detectors.

1. DIRC detectors

The PANDA target spectrometer (see Fig. 1) is almost hermetically sealed to avoid solid angle gaps, and to keep material volume low, there is little spare space inside. The possibility of using thin radiators and placing the readout elements outside the acceptance and potentially outside the magnet return yoke favours DIRC designs to use as Cherenkov imaging detectors for particle identification.

With the momentum ranges anticipated for the physics reactions in PANDA, Figure 2 showing a sample/benchmark reaction, the demands on the separation power increase towards forward angles.

Although the detectors cover different angular ranges, each of the DIRC designs suggested for PANDA nevertheless has to improve over currently implemented DIRC designs, and hence needs to address the effects of chromatic dispersion of the Cherenkov light emission. For the time-of-propagation design selecting a narrow wavelength band limits the group velocity time spread. For the optical imaging design a prism element can largely correct the dispersion angle spread.

The detectors are being located in a high radiation area, proton beam irradiation up to 10Mrad [2] showing that amorphous fused silica is a radiation-hard radiator material. Several photon detector types are tested whether they stand a high magnetic field of

$B \approx 2$ Tesla [3] and high photon rates.

2. Barrel DIRC

The DIRC in the barrel part covers the angular range from $\vartheta=22^\circ$ to 140° . The design is initially based on a scaled version the BaBar DIRC [4]. In order to improve performance, combining the time of arrival of the photons with their spatial image determines not only the particles velocity, but also the wavelength of the photons. Therefore dispersion correction at the lower and upper detection threshold is possible. See the separate paper [5] in these proceedings for details of the PANDA Barrel DIRC.

3. Endcap DIRC position

Two DIRC design options exist for the endcap part of the target spectrometer section. These differ in the photon readout design but both use an amorphous fused silica radiator disc. The endcap detector position covers forward angles up to $\vartheta = 22^\circ$ excluding an inner rectangular acceptance of $\vartheta_x = 10^\circ$ horizontal and $\vartheta_y = 5^\circ$ vertical half-angles.

In such a one-dimensional³ DIRC type a photon is transported to the edge of a circular disc while preserving the angle information. Avoiding too much light scattering loss at the surface reflections requires locally (in the order of millimetres) a surface roughness not exceeding several nanometres RMS.

³ Light is only reflected on surfaces of one spatial orientation, here the two disc surfaces both normal to the z axis.

The lower velocity threshold which is common to both designs depends on the onset of total internal reflection for a part of the photons emitted in the Cherenkov cone.

3.1. Time-of-Propagation disc DIRC

In the Multi-Chromatic Time-of-Propagation design (see separate paper [6] for more detail) small detectors measure the arrival time of photons on the disc rim requiring $\sigma_t=30\text{--}50$ ps single photon resolution.

For any given wavelength the disc edge is effectively covered alternately with mirrors and detectors. Only due to the resulting different light path lengths one can determine accurately enough the start reference time, the time when the initial charged particle enters the radiator and starts creating the Cherenkov photons, as the stored antiproton beam in the HESR has no suitable time structure to be used as an external time start.

As some of the light is reflected several times before hitting a detector, the longer path lengths allow a better relative time resolution.

The use of dielectric mirrors as colour filters allows the use of multiple wavelength bands within the same radiator (the current design suggesting two bands) resulting in higher photon statistics. The narrow wavelength bands minimise the dispersion effects, and the quantum efficiency curve of the photocathode material could be optimised for each wavelength band individually.

3.2. Focusing Lightguide disc DIRC

In the Focusing Lightguide Dispersion-Correcting design (Figures 3 and 4) when a photon arrives at the edge of the circular or polygonal disc it enters into one of about hundred optical elements on the rim. Here the two-fold angle ambiguity (up-down) is lifted, the chromatic dispersion corrected and the photon focussed onto a readout plane. While the optical element entered determines the ϕ coordinate, measuring the position in the dispersive direction on the focal plane of the focusing lightguide yields the θ coordinate.

Lithium fluoride (LiF) is UV transparent and has particularly low-dispersion. Proton beam irradiation of a test sample shows that radiation-produced colour centres are confined to sufficiently small wavelength ranges and only partially absorbing at

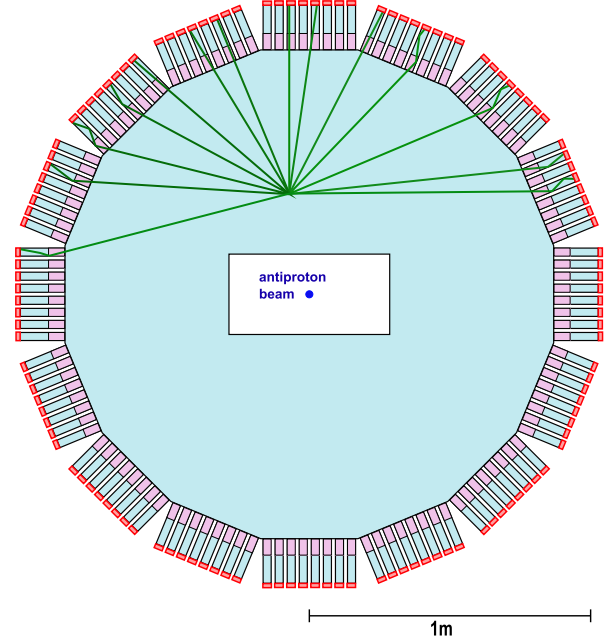


Fig. 3. Polygon disc with focussing lightguides attached to the rim used as optical readout components.

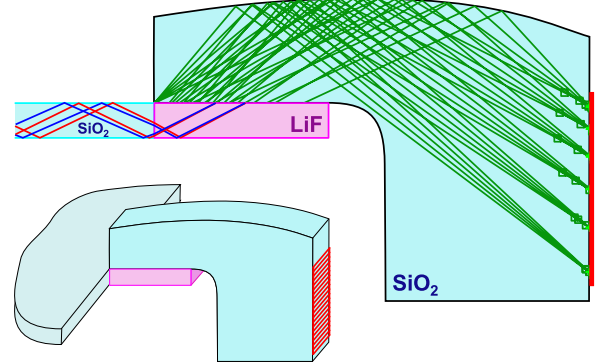


Fig. 4. Lightguide side view (inset 3D-visualisation) shown with a set of rays used for optimising the lightguide curvature. Reflections at the parallel front and back surfaces keep the light inside but do not affect the focussing properties.

the expected PANDA lifetime dose. Hence we think we can use LiF as a prism element (see Figure 4) to correct the Cherenkov radiation dispersion. The two boundary surfaces, with the radiator disc and the subsequent lightguide, make the chromatic dispersion correction angle-independent in first order.

As with the radiator, the light impinging on the inside of the lightguide's curved surface undergoes total internal reflection, hence no mirror coating is needed. The mirror makes the focussing also independent of the wavelength.

With the light staying within the dense optical

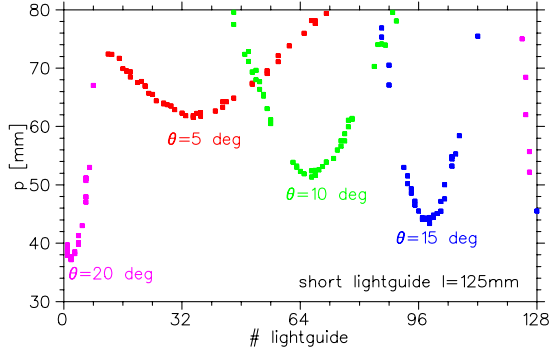


Fig. 5. Simulated photon hit pattern for four particles emitted at different angles θ and ϕ from the target vertex.

material of the lightguide most of the incoming light phase space from the disc is mapped onto the focal plane with its one-coordinate readout. The focussing surface with cylindrical shape of varying curvature has been optimised to give an overall minimum for the focus spot sizes of the different angles on the focal plane, individual standard deviations being well below 1 mm for the instrumented area.

3.3. Optical Simulations

Charged particles emitting cherenkov radiation and photon propagation has been simulated as shown here for the Focussing Lightguide design, and detector resolution derived in analysing the photon hit patterns.

The charged particle trajectory includes angular straggling, and the wavelength dependence of the refractive indices is parametrised with Sellmeier coefficients. Examples of idealisations: perfectly parallel disc surfaces, no bulk light absorption and 100% reflectivity for total internal reflection (can be investigated separately), no detector noise and light from background particles.

The photon pattern analysis is seeded with particle vertex information smeared to the resolution of the upstream tracking detectors. Differential response vectors are computed, one tracking parameter offset at a time, with high photon statistics using the simulation code. Particle vertex parameters and velocity are then fitted simultaneously.

The detector resolving power is then derived from the mean m and standard deviation σ of $\beta = v/c$ of event samples for two different particle types A and B of same momentum, yielding the sigma separation value defined as

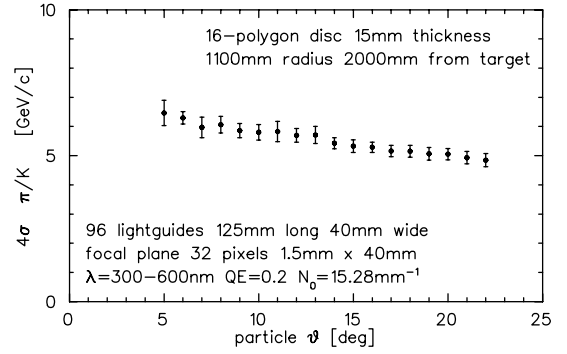


Fig. 6. Simulation-derived pion-kaon separation power for a focusing lightguide design with a 15 mm thick amorphous fused silica disc and 0.4 eV photon detection efficiency.

$$\sigma_{SEP} = \frac{|m_A - m_B|}{\sigma_\beta} = \frac{|m_A - m_B|}{(\sigma_A/2 + \sigma_B/2)}$$

For an Endcap DIRC detector with 96 lightguides and 3072 detector pixels that fits inside the target spectrometer return yoke Figure 6 shows the angle-dependent upper momentum limit being 5–6 GeV/c for 4σ pion-kaon separation within the acceptance $\phi=5^\circ-22^\circ$.

4. Conclusions

The high antiproton rates expected for the PANDA experiment require novel detectors. Current Research and Development addresses the point that the proposed detector components have to stand the harsh environment. We propose several DIRC detector designs for PID that fit into the limited available space of the target spectrometer, and with increased performance over currently running DIRC models meet the physics requirements.

5. Acknowledgements

This work is supported by EU FP6 grant, contract number 515873, DIRACsecondary-Beams.

References

- [1] PANDA Collaboration, Technical Progress Report, FAIR-ESAC/Pbar 2005
- [2] M. Hoek et al., these proceedings
- [3] Albert Lehmann et al., these proceedings
- [4] R. Alexsan et al. Nucl. Instr. Meth. **A397**,261 (1997)
- [5] C. Schwarz et al., these proceedings
- [6] P. Schönmeier et al., these proceedings

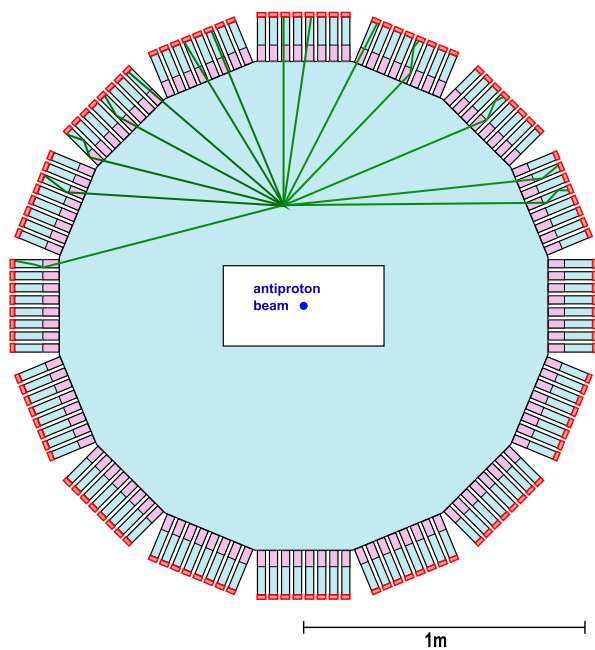


Fig. 7. disc 16 polygon.

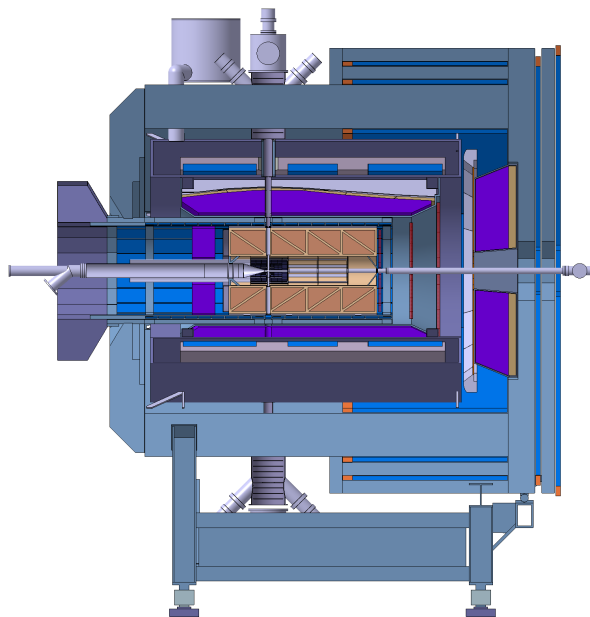


Fig. 10. PANDA target spectrometer

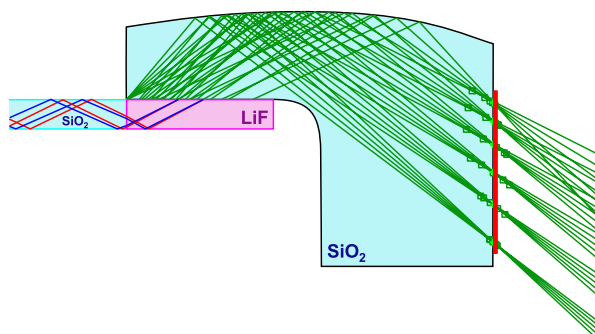


Fig. 8. lightguide side view with rays.

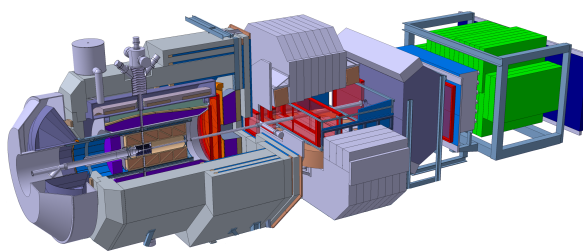


Fig. 11. PANDA spectrometer3d

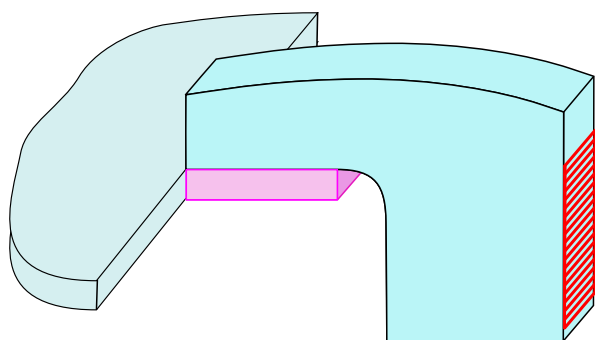


Fig. 9. Lightguide 3d visualisation.

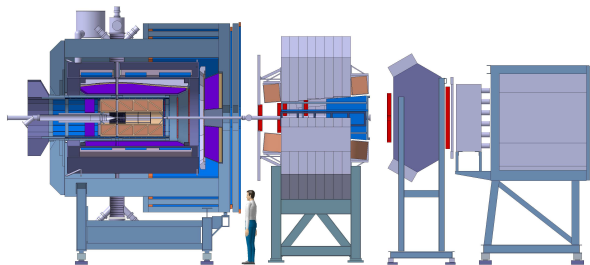


Fig. 12. PANDA spectrometer2d

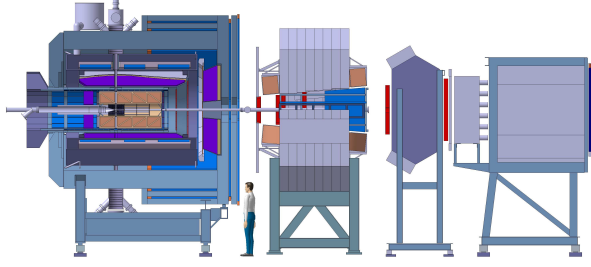


Fig. 13. PANDA spectrometer side view, target spectrometer left, further downstream the dipole in the middle with several forward spectrometer sections to the right.

The RICH detector in the forward spectrometer part will be of a standard aerogel radiator and curved mirror design similar to the HERMES RICH

For the charged particle identification of the PANDA experiment at FAIR, one foresees three imaging Cherenkov detectors. An aerogel detector of standard design will cover the forward spectrometer acceptance.

based on 15mm disc thickness, 96 lightguides with 32 pixels each and 0.4eV ($\epsilon_{QE}=0.2$ for $\lambda=300-600\text{nm}$). The simulation results extend beyond the actual angular coverage.

$p\bar{p} \rightarrow \psi_h \eta$ $\vartheta=22^\circ-140^\circ$, the Endcap DIRC the more forward range $\vartheta=5^\circ=22^\circ$.

Acceptance plot for kaons from the $p\bar{p} \rightarrow \psi_h \eta$ reaction at $p_{\bar{p}}=15\text{ GeV}/c$. The Barrel DIRC covers the range $\vartheta=22^\circ-140^\circ$, the Endcap DIRC the more forward range $\vartheta=5^\circ=22^\circ$.

ingredients: 3d simulation,

Sellmeier parametrisation of refractive indices wavelength dependence, analysis based on photon hit patterns, seeded with smeared Monte Carlo truth vertex equivalent to tracking information, resolution derived from event sample analysis distributions.

ideal geometry ideal light transmission, bulk, full reflectivity (no Fresnel formula yet, photons unpolarised, hard cutoff for non-total internal reflection, no background photons

explain 4 sigma